*Annals of Glaciology* 37 2003
© International Glaciological Society

# Properties of ice crystals in NorthGRIP late- to middle-Holocene ice

Anders SVENSSON,[1] Karen G. SCHMIDT,[1] Dorthe DAHL-JENSEN,[1] Sigfús J. JOHNSEN,[1] Yun WANG,[2] Sepp KIPFSTUHL,[2] Thorsteinn THORSTEINSSON[2,3]

[1]*Department of Geophysics, University of Copenhagen, Juliane Maries Vej 30, DK-2100 Copenhagen, Denmark*
*E-mail: as@gfy.ku.dk*

[2]*Alfred Wegener Institute for Polar and Marine Research, P.O. Box 120161, D-27515 Bremerhaven, Germany*

[3]*Science Institute, University of Iceland, Dunhaga 3, IS-107 Reykjavík, Iceland*

ABSTRACT. Detailed measurements of crystal outlines and fabrics have been performed on 35 000 crystals in fifteen $10 \times 20\ cm^2$ vertical thin sections from the North Greenland Icecore Project (NorthGRIP) ice core, evenly distributed in the depth interval 115–880 m. The crystals exhibit important changes over this period. As the ice gets older the mean crystal area increases towards a constant value, the shape of the crystals becomes increasingly irregular, and the area distribution of crystals develops from a single lognormal distribution into a bimodal lognormal distribution. The *c*-axis fabric of the ice shows a smooth development of an increasingly stronger vertical fabric with depth, and the formation of a weak vertical girdle. Already in the younger samples the fabric is rather strongly oriented towards vertical. The fabric and the area of individual crystals are found not to correlate. A simple model, which takes into account the vertical strain of the ice, is applied in an attempt to determine the crystal growth rate at NorthGRIP.

## INTRODUCTION

The Greenland Icecore Project (GRIP) and Greenland Ice Sheet Project 2 (GISP2) deep ice cores were drilled right at the Summit and just 30 km to the west of the Summit of the Greenland ice sheet. The texture (crystal size and shape) and fabric (crystal orientation) of the GRIP and GISP2 ice cores have been discussed in Thorsteinsson and others (1997) and in Gow and others (1997), respectively. For the Holocene part of those cores it is established that crystals grow with age towards a limiting crystal size where polygonization counteracts growth. The *c*-axis fabric develops from a more-or-less random orientation in the shallow ice towards an increasingly strong vertical orientation in the deeper ice.

The North Greenland Icecore Project (NorthGRIP) drilling site is located on an ice ridge 325 km north-northwest of Summit (Dahl-Jensen and others, 2002). At NorthGRIP, conditions are quite similar to those at the Summit sites, except for the location on a ridge rather than on a divide at Summit, and the annual accumulation is 19.5 cm at NorthGRIP compared to 23 cm at GRIP. The mean annual temperature is −32°C at both locations. At NorthGRIP we thus expect ice crystal properties in the upper part of the ice sheet to be similar to those established for the Summit cores. The NorthGRIP fabric has been investigated by Wang and others (2002), who determined the major difference in fabric in comparison to the Summit cores to be the evolution of a vertical girdle fabric with depth due to the stress field on a ridge.

In this study, we focus on the late- to middle-Holocene part of the NorthGRIP ice core, approximately the last 5300 years. We determine crystal outlines and *c*-axis orientations with good statistics using a new Australian ice-crystal analyzer and new imaging software. The purpose of the study is to determine the temporal development in growth, shape and fabric of the crystals, and also to investigate a possible relation between crystal sizes and *c*-axis orientations.

## METHODS

Fifteen vertical samples, 20 cm long, 10 cm wide and 0.7 cm thick, were obtained from the NorthGRIP ice core, evenly distributed in the depth interval 115–880 m. From each of these, two $10 \times 10\ cm^2$ vertical thin sections were prepared using standard techniques (Hansen and others, 2002). The mean annual-layer thickness at NorthGRIP is 19.5 cm, so by taking 20 cm long samples we attempt to average out the quite important seasonal variability in crystal properties (Svensson and others, 2003). The orientation of the vertical sections with respect to the core axis is not known.

The fabric and the outline of the crystals were determined on a new Australian automatic crystal analyzer in Copenhagen using the procedures described in Svensson and others (2003). For each crystal the following parameters were determined: area, width, height, flattening, roundness and *c*-axis orientation. The crystal areas are obtained by counting the number of pixels within the individual crystal boundaries from the digital sample images. The width and the height of a crystal are defined as the width and the height of the crystal's bounding box, the bounding box being the smallest rectangle with horizontal and vertical sides which completely embody the crystal. The crystal's flattening is given as the width-to-height ratio of the bounding box. The roundness $r$ of a crystal with perimeter $P$ and



https://doi.org/10.3189/172756403781815636 Published online by Cambridge University Press

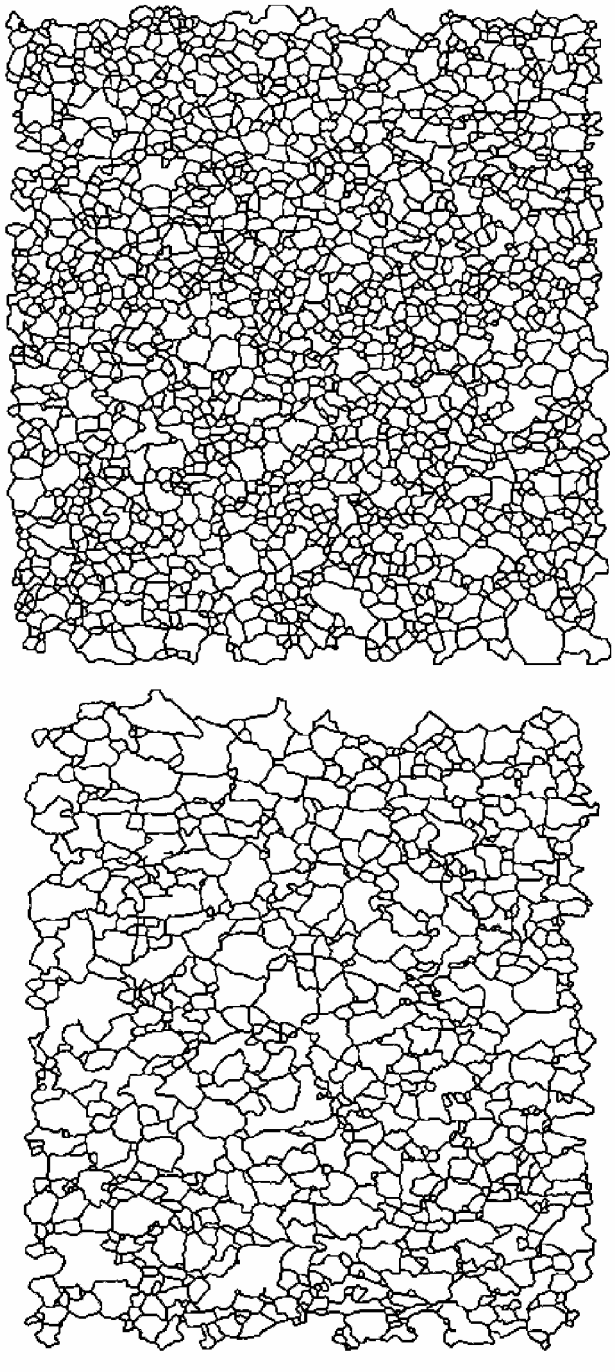

*Fig. 1. Crystal outlines of two thin sections. The top of the core is up in the figure. The upper section is from 165 m depth and contains 2014 crystals, while the lower section is from 825 m depth and holds 870 crystals.*

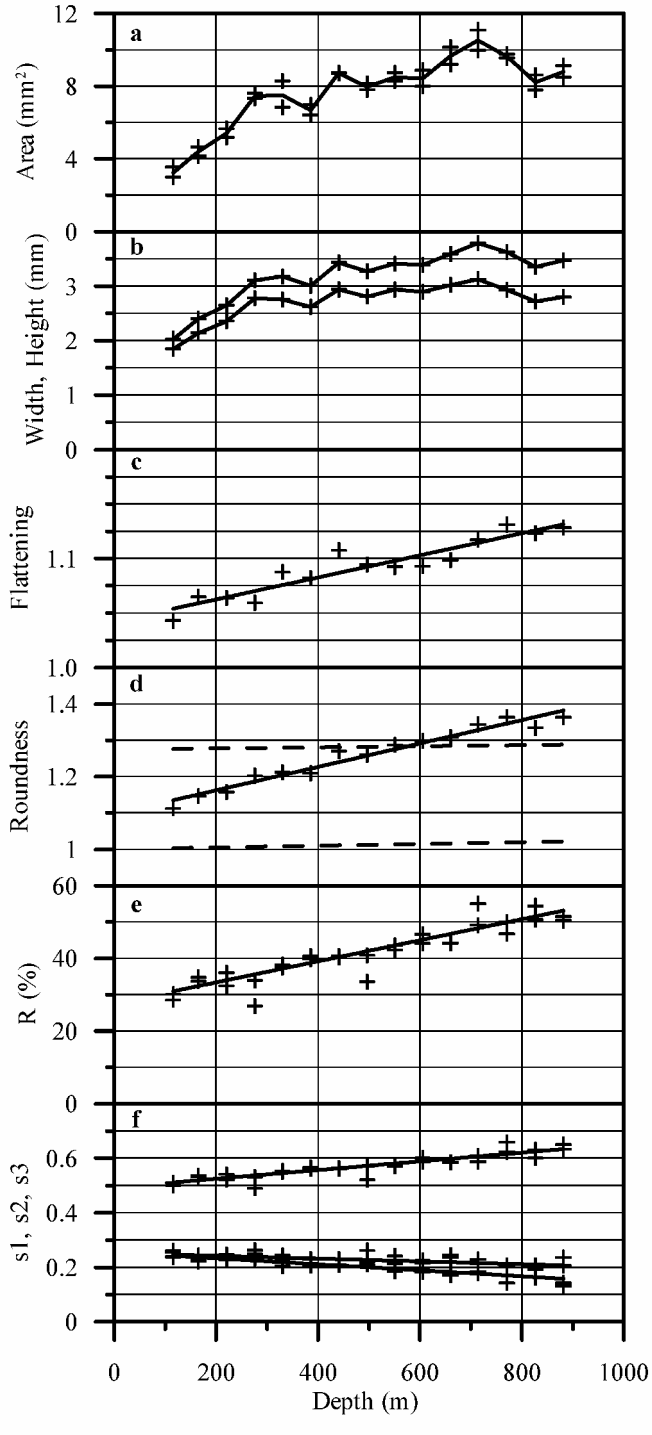


*Fig. 2. (a) The mean crystal area of individual thin sections (points) and the average value of each twin pair of thin sections (curve). (b) The average horizontal width (upper curve) and vertical height (lower curve) of the crystal's bounding box. (c) The ratio of crystal width to crystal height (points) and a linear fit function (curve). (d) The average roundness of crystals (points) and a linear fit (full curve). The roundness of an ellipse (lower dotted curve) and of a rectangle (upper dotted curve) with the same flattening as the crystals is indicated. (e) The degree of orientation of c axes of individual thin sections (points) and a linear fit function omitting the outliers at 275 and 495 m depth, respectively (curve). (f) The normalized eigenvalues s1–s3 of individual thin sections (points) and corresponding linear fit functions (curves).*

area $A$ is defined as $r = P^2/(4\pi A)$. Roughly, the roundness is a measure of the complexity of the outline of the crystal. A circle has the lowest possible roundness value of unity, while a square has a roundness of $4/\pi \approx 1.27$. For each thin section the degree of orientation of $c$ axes ($R$) and the normalized eigenvalues of orientation (s1, s2, s3) were obtained. These parameters are defined and discussed in a NorthGRIP context in Wang and others (2002).

## RESULTS

The outlines of 35 000 complete crystals were identified in the 30 thin sections, and the $c$-axis orientation was determined for >95% of these. Figure 1 shows examples of the crystal outlines as determined in two thin sections. The $c$-axis orientation could not be determined for crystals that have significant overlap with other crystals in the thin section.



https://doi.org/10.3189/172756403781815636 Published online by Cambridge University Press

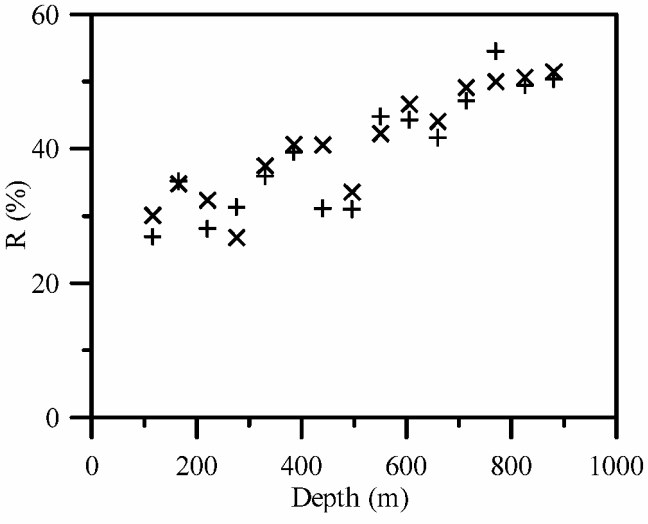


*Fig. 3. The degree of orientation of c axes (R) as determined by the Japanese c-axis analyzer at AWI (pluses) and on the Australian instrument in Copenhagen (crosses). Measurements are performed on the same samples, but the AWI measurements include only about 25% of the crystals in each sample.*

The variability of important crystal properties with depth is shown in Figure 2. The mean crystal area displays a general but not very regular increase with depth, leading to a limiting value for the older samples of around 10 $mm^2$. Because each of our samples covers approximately one annual layer, the influence of the seasonal variability in crystal area will almost be averaged out. The difference in mean crystal area between two adjacent thin sections, each representing about half a year, gives an estimate of the order of magnitude of the seasonal variability. Such pairs of thin sections are shown as two points corresponding to the same depth in Figure 2.

The average crystal width and height both follow the pattern of the mean crystal area closely, and generally the crystal sizes are in quite good agreement with those obtained for the Summit ice cores (Gow and others, 1997; Thorsteinsson and others, 1997). The crystal flattening, defined as the crystal width divided by the crystal height, increases almost linearly over the entire depth range, reaching a maximum of 1.12 at 880 m depth. The roundness parameter, which is a measure of the complexity of the crystal outline, increases almost linearly from close-to-circular values for the youngest samples to higher-than-rectangular values for the oldest samples.

The degree of orientation of *c* axes, the *R* parameter, is found to increase almost linearly with depth, from about 30% at 115 m depth to around 50% at 880 m depth. A sample with randomly distributed *c*-axis orientations has $R = 0\%$, while a single-maximum fabric has $R = 100\%$. The *R* values at 275 and 495 m depth, which deviate from the general trend, have been confirmed by remeasurement. The three eigenvalues of orientation, s1–s3, also display a close to linear depth dependence. s3 increases following the trend of *R*, while s1 and s2 start out at the same value at 115 m depth, and then split and decrease slightly with depth.

Wang and others (2002) published results from a study of fabric evolution at 100–2930 m depth in the NorthGRIP core, carried out at the Alfred Wegener Institute for Polar and Marine Research (AWI). A new copy of the Japanese automatic ice-fabric analyzer (Wang and Azuma, 1999) was used in that study. The results presented here for the depth interval

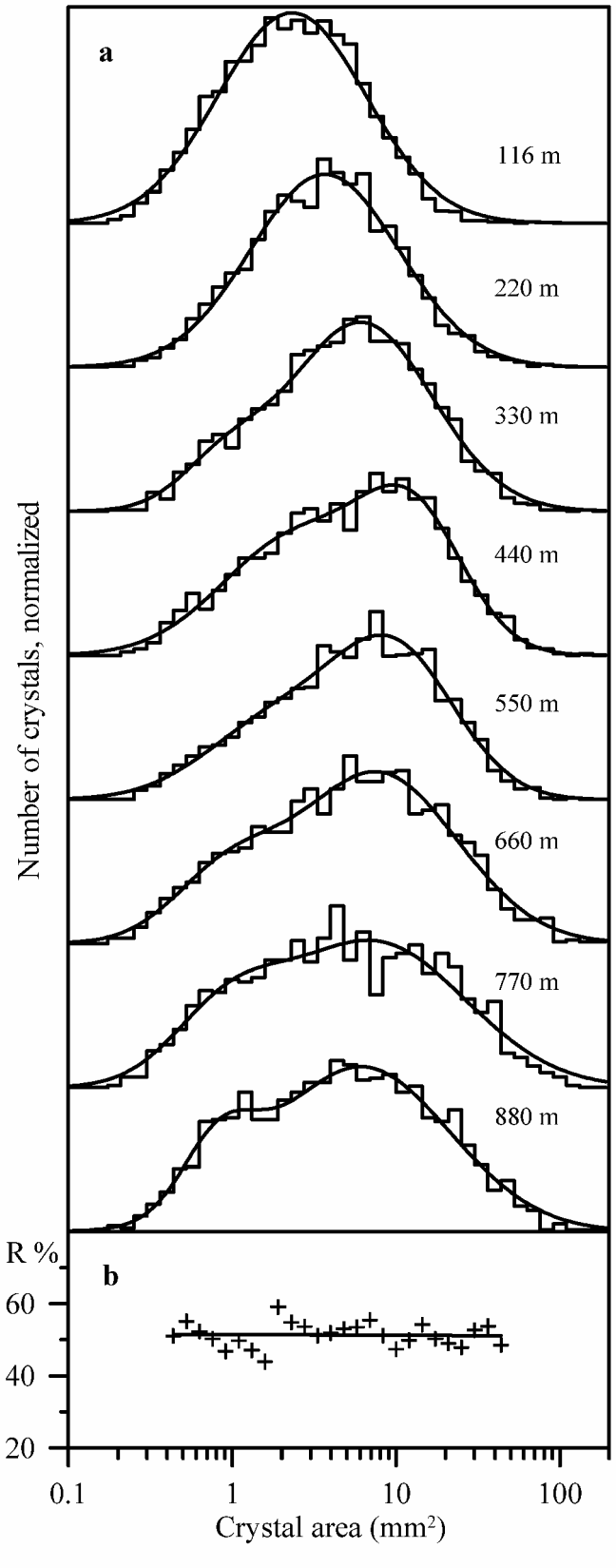


*Fig. 4. (a) Normalized crystal area distributions at eight depths, which are indicated (step curves). The distributions at 116 and 220 m depth are fitted with a single lognormal function; the following distributions are fitted with bimodal lognormal functions. (b) The degree of orientation of c axes (R) as a function of crystal area for samples from below 700 m depth (points) and a linear fit (curve).*

115–880 m are not in good agreement with those of Wang and others (2002), who obtain generally lower values for the degree of orientation (*R*) in this depth interval. In addition, their



https://doi.org/10.3189/172756403781815636 Published online by Cambridge University Press

results indicate a sudden jump to higher values of $R$ (and corresponding changes in the other statistical parameters) at 750 m depth. Following publication, it was discovered that the unusual results obtained by Wang and others (2002) in the interval 100–800 m were due to a software error, which was corrected before measuring the samples below 800 m. While this disagreement was being studied, it was decided to perform a comparative study, in which some of the thin sections used in this study were remeasured at AWI on the instrument used by Wang and others (2002), after the software error had been corrected. Due to differences between the two instruments, it was not possible to measure the same number of crystals in each sample. In Copenhagen, about 95% of all crystals in the samples were measured, whereas the AWI instrument included about 25% of the crystals in the measurement. In Figure 3 the $R$ parameter is compared for the two measurement series. The results are in quite good agreement, and, except for one section (at 440 m depth), the $R$ values agree within 5%. We conclude that the results on fabric statistics presented in Figure 2 can be considered reliable, and that the software error in the AWI instrument has been satisfactorily corrected.

The development of the crystal area distribution with depth is presented in Figure 4a. The distribution evolves from a single lognormal distribution in the upper hundreds of meters to a bimodal distribution at greater depths. In Figure 4b, the $R$ parameter for the samples from below 700 m depth is shown as a function of crystal area. The $R$ parameter displays no correlation with crystal areas.

## DISCUSSION

### Crystal areas

Some fluctuations away from the general trend of growth toward the limiting value is observed for the crystal areas in Figure 2a. One could argue that because the NorthGRIP core is drilled on an ice ridge, the horizontal width of the crystals, and hence the cross-sectional area of the crystals, will depend on the orientation of the vertical section with respect to the core axis. Since the horizontal strain of the ice is almost entirely in the direction perpendicular to the ridge (Wang and others, 2002), the crystals in a section with this orientation will be more elongated horizontally than those of a section oriented parallel to the ridge. The crystal height, however, will not be influenced by this effect. In Figure 2b, the average crystal height is seen to correlate with both crystal area and crystal width. We therefore conclude that the varying orientation of the samples with respect to the core axis does not importantly influence the variability in crystal areas. This varying orientation of the samples may, however, explain the deviation in crystal flattening away from the general trend in Figure 2c. Other possible reasons for the fluctuations in mean crystal areas would be an interannual variability in the amount of impurities of the ice, or deviations from the mean annual-layer thickness of the sampled sections. The impurity content of the sampled ice has, however, not been measured, and the exact annual-layer thickness of the sampled ice is not known.

Figure 4 shows how the crystal area distribution in the younger samples starts out as a single log-normal mode, which moves towards larger crystals until a depth of 400–500 m. Starting at about the same depth, a second mode of smaller crystals appears, which displays increasing amplitude with time. A possible explanation for the formation of this second mode in the older samples is that the crystals become more and more irregular with age. This is illustrated in Figure 1, where the crystal outlines of a young and an old sample can be compared. The older sample contains the larger crystals of the two, and the crystals in the older sample are much more irregular. A line put across the younger section is unlikely to hit the same crystal more than once, because most of the crystals have regular shapes. In the older sample, a cross-sectional line has a greater chance of hitting several crystals more than once, because those crystals are more gnarled. The same effect occurs when a two-dimensional thin section is obtained from ice composed of crystals which may have a rather complex shape in three dimensions (Rigsby, 1968; Nishida and Narita, 1996). The complicated shape of the older crystals may cause some of them to appear several times in the thin sections, the so-called duplication effect. The increasing irregularity of the crystals with age is reflected by the steady increase of the roundness parameter (Fig. 2d). That the crystals do not continue growing with depth is thought to be due to a polygonization effect, which counteracts the growth (Alley, 1992; Thorsteinsson and others, 1997).

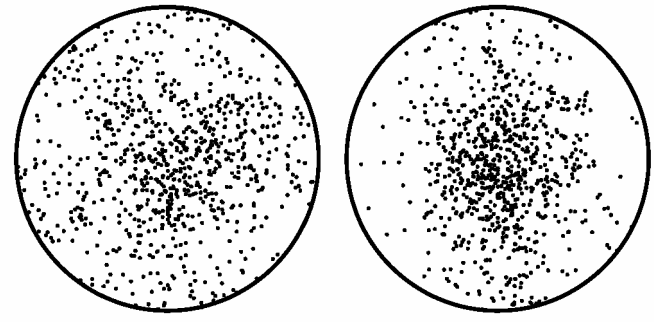

*Fig. 5. Schmidt diagrams, each showing 800 randomly selected c axes in a horizontal projection, viewed from above. The left diagram shows a sample from 115 m depth with $R = 30\%$ and cylindrical symmetry with $s1 = s2 = 0.25$. The right diagram shows a sample from 880 m depth with $R = 51\%$, which displays a weak girdle with $s1 = 0.13$ and $s2 = 0.24$.*

### Fabrics

The *c*-axis fabric of the late-Holocene part of the NorthGRIP ice core evolves very smoothly. In contrast to the mean crystal area, which exhibits a rather bumpy behavior (Fig. 2a), both the $R$ parameter and the eigenvalues s1–s3 vary almost linearly with depth (Fig. 2e and f). That the $R$ parameter starts out at a value of 30% already at 115 m depth means that some orientation of *c* axes takes place at shallow depth. The slight splitting of the eigenvalues s1 and s2 with depth is due to the development of a vertical girdle fabric, which occurs because NorthGRIP is located on an ice ridge, and which is much more prominent deeper in the ice (Wang and others, 2002). Already at 880 m depth, however, the girdle can be seen in the fabrics diagram in Figure 5. The $R$ parameter shows no correlation with the crystal area (Fig. 4b). That is, crystal growth and strengthening of the fabric seem to develop independently in the ice. This argument is in agreement with the work of Svensson and others (2003), in which no correlation between fabric and crystal area is observed on a seasonal time-scale.



https://doi.org/10.3189/172756403781815636 Published online by Cambridge University Press

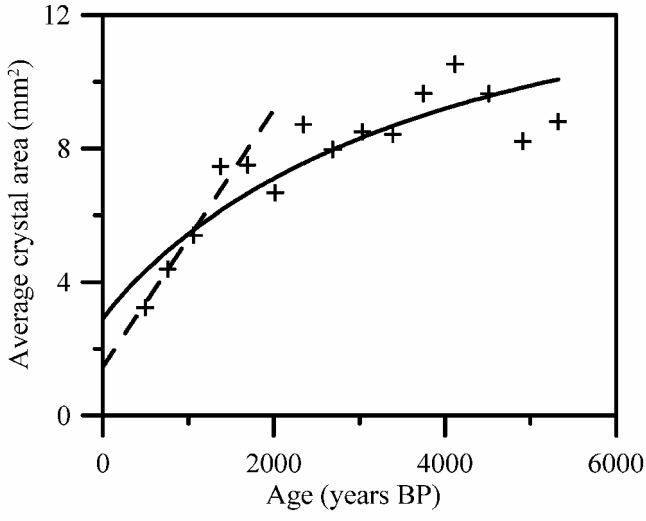


*Fig. 6. The mean crystal areas on a time-scale (points), a linear normal grain-growth fit (Equation (1), $n = 2$) for the interval 0–2000 years (dotted curve), and a strained normal grain-growth fit (Equation (4), $n = 3$) for the entire depth interval (full curve).*

## Crystal growth

In the context of Greenland ice crystal texture, the late-Holocene part of the ice sheet is often termed the normal grain-growth regime (Alley, 1992), because the ice crystals in this part of the ice sheet grow linearly with time $t$, according to the law:

$$l^n = l_0^n + k_n t \quad \text{or} \quad \frac{\mathrm{d}l^n}{\mathrm{d}t} = k_n \,, \tag{1}$$

where $l$ is a measure for the crystal size, $l_0$ is a constant yielding the initial crystal size, $k_n$ is the crystal growth rate and $n$ is a dimensional constant. Generally, $k_n$ depends on factors like temperature and the amount of impurities in the ice, but because of the stable Holocene climate in Greenland, $k_n$ can be assumed constant at a given location. For ice, $n$ is often set equal to two, meaning that the crystal areas grow linearly with time.

Figure 6 shows the average crystal areas on a time-scale, which is established from correlation with volcanic horizons in the NorthGRIP core that are previously dated in other Greenland ice cores. For the last approximately 2000 years, the crystal growth is seen to be linear with time and thus following the normal grain-growth law, Equation (1) with $n = 2$. From a linear fit to the data points, we determine a crystal-area growth rate of $k_2 = 3.85 \times 10^{-3}$ mm$^2$ a$^{-1}$. Although this growth rate does not take into account the sectioning effect — the fact that the thin section usually does not cut through the maximum extent of each crystal — we prefer to report this rate, because it is obtained directly from the measured crystal areas without any corrections. Thorsteinsson and others (1997) determined a crystal growth rate for the GRIP ice core of $k_2 = 5.6 \times 10^{-3}$ mm$^2$ a$^{-1}$. They used a correction factor of 1.5 for crystal areas, derived from linear intercept measurements of crystal diameters of each ice crystal. If we apply the same correction factor for the present study, we obtain a crystal growth rate in very good agreement with that of Thorsteinsson and others (1997).

It is clear that for the ice older than 2000 years the crystal areas no longer grow linearly with time, but merely approach a constant crystal size (Fig. 6). The reason for this is probably a combination of the vertical strain of the ice, which causes a flattening of the crystals with depth, and the crystal polygonization. In the following, we will extend the normal grain-growth model to take into account vertical strain. Let $l$ in Equation (1) be a measure of the vertical size of the crystals. From the definition of the vertical strain rate $\dot{\varepsilon}_z$ we get:

$$\frac{l^n}{l}\frac{\mathrm{d}l}{\mathrm{d}t} = l^n \dot{\varepsilon}_z \quad \text{or} \quad \frac{\mathrm{d}l^n}{\mathrm{d}t} = n l^n \dot{\varepsilon}_z \,. \tag{2}$$

For the late Holocene, $\dot{\varepsilon}_z$ can be assumed to be constant, and from the thinning of the annual layers it is estimated to have a magnitude of $\dot{\varepsilon}_z = -7.4 \times 10^{-5}$ a$^{-1}$. In combining Equations (1) and (2) we obtain an expression for the vertical crystal size, which takes into account both normal grain growth and the vertical strain of the ice:

$$\frac{\mathrm{d}l^n}{\mathrm{d}t} = n l^n \dot{\varepsilon}_z + k_n \,. \tag{3}$$

We will call this strained normal grain growth. The solution to Equation (3) is given by

$$l^n = l_\infty^n [1 - \exp(-t/\tau_n)] + l_0^n \exp(-t/\tau_n) \,, \tag{4}$$

where $\tau_n = -(n\dot{\varepsilon}_z)^{-1}$ is the crystal-growth time constant, and $l_\infty = \sqrt[n]{k_n \tau_n}$ is the crystal-size limiting value. The vertical crystal size, $l$ in the above, is not a uniquely defined quantity. It could be the crystal height as defined in this study, or it could be the diameter or the major axis of a best-fit ellipse to the crystal. Because we prefer to apply the model to a directly measured quantity, it is more convenient to work with crystal area than with crystal size. We thus define $l^2$ to be crystal area, although this is not completely in accordance with the model assumptions. The best fit to the crystal area profile with Equation (4) is obtained for $n = 3$, which yields $k_3 = 9.75 \times 10^{-3}$ mm$^3$ a$^{-1}$ (Fig. 6). Although this fit does not reproduce data very well, the strained model does produce a better overall fit to the crystal area profile than does the normal grain-growth model. The fact that the best fit is obtained for $n = 3$ raises the question whether the crystal volume rather than the cross-sectional crystal area better describes the physical conditions dictating crystal growth at depths below the breakdown of the normal grain-growth model.

## CONCLUSIONS

The crystal outline and fabric have been determined in 15 twin pairs of vertical thin sections from the NorthGRIP ice core covering approximately the last 5300 years.

The crystal area distribution develops with depth from a single lognormal mode into a bimodal lognormal function. We propose that the appearance of the second mode of smaller crystals is related to a duplication effect in the older samples (e.g. that the same crystal appears more than once, because the crystals are becoming increasingly irregular with time). This argument is supported by the increase of the crystal roundness parameter with time.

For the fabric, we conclude that the degree of orientation of $c$ axes increases linearly from around 30% at 115 m depth to around 50% at 880 m depth and that a weak girdle in the fabrics diagram is forming in the deeper samples. The $c$-axis orientation seems completely independent of crystal size.

Concerning crystal growth, we find that a normal grain-growth model can fit the mean crystal area profile in the upper 350 m of the ice, but that an extended grain-growth model, which takes into account the vertical strain of the ice, better reproduces the entire crystal area profile. This



https://doi.org/10.3189/172756403781815636 Published online by Cambridge University Press

model suggests that below a certain depth it may be the crystal volume rather than the crystal area in a cross-section that grows linearly with time.

## ACKNOWLEDGEMENTS

We are grateful to A. K. Alsing, L. W. Bjerrum, and T. F. Nielsen for help with the sampling and data processing. This work is a contribution to the North Greenland Icecore Project, which is directed and organized by the Department of Geophysics at the Niels Bohr Institute for Astronomy, Physics and Geophysics, University of Copenhagen. The NorthGRIP program is supported by funding agencies in Denmark, Belgium, France, Germany, Iceland, Japan, Sweden, Switzerland and the U.S.A.

## REFERENCES

Alley, R. B. 1992. Flow-law hypotheses for ice-sheet modeling. *J. Glaciol.*, **38**(129), 245–256.

Dahl-Jensen, D. *and 8 others*. 2002. The NorthGRIP deep drilling programme. *Ann. Glaciol.*, **35**, 1–4.

Gow, A. J. *and 6 others*. 1997. Physical and structural properties of the Greenland Ice Sheet Project 2 ice cores: a review. *J. Geophys. Res.*, **102**(C12), 26,559–26,575.

Hansen, K. M., A. Svensson, Y. Wang and J. P. Steffensen. 2002. Properties of GRIP ice crystals from around Greenland interstadial 3. *Ann. Glaciol.*, **35**, 531–537.

Nishida, K. and H. Narita. 1996. Three-dimensional observations of ice crystal characteristics in polar ice sheets. *J. Geophys. Res.*, **101**(D16), 21,311–21,317.

Rigsby, G. P. 1968. The complexities of the three-dimensional shape of individual crystals in glacier ice. *J. Glaciol.*, **7**(50), 233–251.

Svensson, A., P. Baadsager, A. Persson, C.S. Hvidberg and M.-L. Siggaard-Andersen. 2003. Seasonal variability in ice crystal properties at NorthGRIP: a case study around 301 m depth. *Ann. Glaciol.*, **37** (see paper in this volume).

Thorsteinsson, Th., J. Kipfstuhl and H. Miller. 1997. Textures and fabrics in the GRIP ice core. *J. Geophys. Res.*, **102**(C12), 26,583–26,599.

Wang Yun and N. Azuma. 1999. A new automatic ice-fabric analyzer which uses image-analysis techniques. *Ann. Glaciol.*, **29**, 155–162.

Wang, Y., T. Thorsteinsson, J. Kipfstuhl, H. Miller, D. Dahl-Jensen and H. Shoji. 2002. A vertical girdle fabric in the NorthGRIP deep ice core, North Greenland. *Ann. Glaciol.*, **35**, 515–520.



https://doi.org/10.3189/172756403781815636 Published online by Cambridge University Press